

Generation of Broad-Band Chaos Using Blocking Oscillator

Nikolai F. Rulkov and Alexander R. Volkovskii

Abstract—In this paper, we discuss fundamentals for the design of a source of chaotic signals based on a blocking oscillator circuit. We study a modification of a well-known circuit of blocking oscillator which leads to the onset of chaotic oscillations. The output signal of such chaotic oscillator is a series of short term pulses characterized by chaotic fluctuations of time intervals between pulses. Such chaotic pulse signals possess a broad-band continuous power spectrum and short correlation length. We discuss the results of theoretical and experimental studies of nonlinear dynamics of the chaotic blocking oscillator.

Index Terms—Bifurcations, chaos, nonlinear circuits.

I. INTRODUCTION

INTENSIVE studies of possible applications of chaotic signals are supported in part by the abilities of simple inexpensive electrical circuits to generate complex chaotic signals. Quite a few simple autonomous nonlinear circuits that possess chaotic dynamics have been proposed and studied, see for example [1]–[6]. Most of these nonlinear circuits produce chaotic signals in form of quasiharmonic oscillations. Chaos in such circuits occurs through bifurcations from a regime of harmonic oscillation. The shape of the power spectrum of such chaotic signals depends upon the amplitudes of higher harmonics which occur due to nonlinear distortions of the original harmonic oscillation. Amplitudes of these harmonics change significantly as the regime of chaotic behavior changes. As the result the broad-band power spectrum of output chaotic signal in these circuits is usually hard to shape unless additional filters are used.

A different approach to generation of chaotic signals is based on utilization of pulse generators which are triggered to produce short pulses at the chaotic moments of time. In this case the shape of the pulses is independent of the oscillation regime of the chaos oscillator that triggers the short pulses. This property of chaotic pulse generator enables one to shape the power spectrum and the autocorrelation function of the chaotic output. Different designs of the chaotic pulse generators were discussed recently in [7]–[11]. The studies of these chaotic pulse generators were motivated by utilization of such circuits in chaos based communication systems. Examples of such communication schemes and advantages of using chaotic pulse signals in-

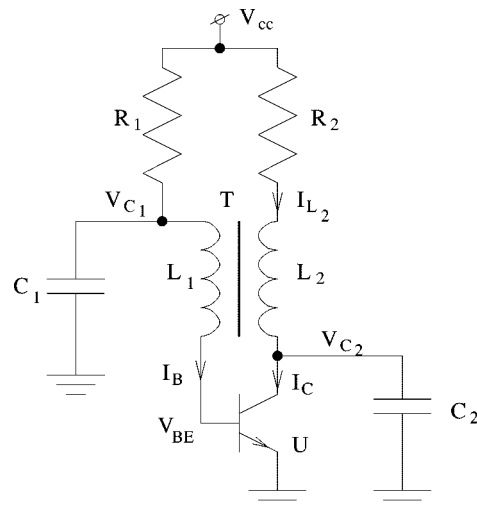


Fig. 1. Chaotic blocking oscillator circuit.

stead of quasiharmonic chaotic signals are discussed in details in [10], [12], [13].

The core of the chaotic pulse oscillators is a circuit that generates time intervals in accordance with the iterations of a chaotic map. Usually, the chaotic map circuit is implemented with a few of integrated circuits such as timers or sample and hold circuits. In this paper, we describe a nonlinear circuit with chaotic behavior which is built on one transistor and very suitable for designing the simple chaotic pulse generators.

The circuit that we propose is a modification of well-known *blocking oscillator* circuit which is used for generation of short periodic pulses. The modification includes a capacitor C_2 added to the collector circuit of blocking generator, see Fig. 1. The additional capacitor C_2 and the inductor L_2 of the transformer T form a resonant circuit, which produces damped oscillation of the current in the transformer excited by the pulses generated in blocking oscillator. This oscillation modulates the voltage at the base of the transistor and influences the conditions for generating the next pulse. We will show how this influence can lead to the onset of chaotic pulsations.

II. DIFFERENTIAL EQUATIONS FOR THE CHAOTIC BLOCKING OSCILLATOR

The analysis of the nonlinear dynamics of the original blocking oscillator is a classical problem of the nonlinear oscillations theory and can be found in the textbooks. To derive the equations for the chaotic blocking oscillator we will follow the book [14]. We consider the schematic illustrated in Fig. 1.

Manuscript received April 26, 2000; revised January 29, 2001. This research was supported in part by the Army Research Office under Grant DAAG55-98-1-0269, and in part by the U.S. Department of Energy, Office of Basic Energy Sciences, under Grant DE-FG03-90ER14138. This paper was recommended by Associate Editor C. K. Tse.

The authors are with the INLS, University of California at San Diego, La Jolla, CA 92093-0402 USA.

Publisher Item Identifier S 1057-7122(01)04288-X.

The equations for the voltages across the capacitors C_1 and C_2 where can be written in the form

$$R_1 C_1 \frac{dV_{C_1}}{dt} = V_{cc} - V_{C_1} - R_1 I_B \quad (1)$$

$$R_2 C_2 \frac{dV_{C_2}}{dt} = V_{cc} - V_{R_2} - R_2 I_C \quad (2)$$

where I_B is the current through the base of the transistor and I_C is the current through the collector. These currents can be modeled by nonlinear functions of the voltage V_{BE} across the base-emitter junction of the transistor, and the voltage $V_{CE} = V_{C_2}$ between the collector and emitter. We will describe the characteristics of the transistor by the functions $I_B = g(V_{BE})$ and $I_C = f(V_{BE}, V_{C_2})$.

In practice, to generate rectangular pulses with sharp edges, it is necessary that transformer has small magnetic leakage flux and small stray capacitance across the windings. It is natural to assume as a first approximation that magnetic leakage flux is zero. With this assumption the magnetic flux through each turn of any of the winding is determined by the total number of ampere-turns in all windings and is given by

$$\Phi = \frac{L_1}{n_1} (I_B - k I_{L_2}) \quad (3)$$

where I_{L_2} is the current flowing in the winding of the inductor L_2 , $k = n_2/n_1$ is the voltage ratio of the L_2 winding with respect to the L_1 winding, n_1 and n_2 are the number of turns in the windings L_1 and L_2 , respectively. In (3), we took in to account that L_1 and L_2 windings of the transformer are so connected that partial magnetic fluxes generated in the transformer by the positive currents I_B and I_{L_2} have opposite sign. This is required to provide positive feedback and achieve self-exciting oscillations in the circuit. Let us introduce the magnetization current of the transformer

$$I_M = I_B - k I_{L_2}. \quad (4)$$

Then, the induced electromotive forces (EMFs) in the L_1 and L_2 windings of the transformer will be, respectively

$$-\frac{d}{dt} (n_1 \Phi) = -L_1 \frac{dI_M}{dt} \quad \frac{d}{dt} (n_2 \Phi) = k L_1 \frac{dI_M}{dt}. \quad (5)$$

Using (5), the equations for the transformer can be written in the form

$$-L_1 \frac{dI_M}{dt} = V_{BE} - V_{C_1} = (V_{R_2} - V_{C_2})/k. \quad (6)$$

Substituting (4) we find

$$I_M = g(V_{BE}) - k \frac{V_{cc} - V_{R_2}}{R_2} \quad (7)$$

and eliminating the voltage V_{R_2}

$$V_{R_2} = k(V_{BE} - V_{C_1}) + V_{C_2} \quad (8)$$

we rewrite (6) in the following form:

$$L_1 G(V_{BE}) \frac{dV_{BE}}{dt} - \frac{k^2 L_1}{R_2} \frac{dV_{C_1}}{dt} + \frac{k L_1}{R_2} \frac{dV_{C_2}}{dt} = -V_{BE} + V_{C_1} \quad (9)$$

$$G(V_{BE}) = \frac{dg(V_{BE})}{dV_{BE}} + \frac{k^2}{R_2}. \quad (10)$$

Solving (1), (2), and (9) for the time derivatives, we obtain the equations of the circuit in the form

$$R_1 C_1 \frac{dV_{C_1}}{dt} = V_{cc} - V_{C_1} - R_1 g(V_{BE}) \quad (11)$$

$$R_2 C_2 \frac{dV_{C_2}}{dt} = V_{cc} - V_{C_2} - k(V_{BE} - V_{C_1}) - R_2 f(V_{BE}, V_{C_2}) \quad (12)$$

$$L_1 G(V_{BE}) \frac{dV_{BE}}{dt} = S_2 \left(\frac{R_2 C_2}{R_1 C_1} - \frac{1}{k} \right) V_{cc} + (1 - S_1 - S_2) V_{C_1} + \frac{S_2}{k} V_{C_2} - \left(1 - \frac{S_2}{k} \right) V_{BE} - S_1 R_1 g(V_{BE}) + \frac{S_2 R_2}{k} f(V_{BE}, V_{C_2}) \quad (13)$$

where

$$S_1 = \frac{k^2 L_1}{R_2 R_1 C_1} \quad S_2 = \frac{k^2 L_1}{R_2^2 C_2}. \quad (14)$$

This system of differential equations represent a complete set of the state equations for the nonlinear circuit shown in Fig. 1. Deriving these equations we neglected small stray capacitance of across the windings of the transformer, small magnetic leakage flux and nonlinearities in the transformer.

Despite the neglected parasitic parameters the oscillations produced by this three-dimensional model are very similar to the behavior of real circuit. To demonstrate that we integrated numerically system (11)–(13). In the simulations we approximated the nonlinearities of the transistor by the functions $g(V_{BE}) = I_S \exp(V_{BE}/V_T)$, and

$$f(V_{BE}, V_{C_2}) = h g(V_{BE}) \times \begin{cases} V_{C_2}/10, & \text{if } V_{C_2} < 0 \\ 10V_{C_2}, & \text{if } 0 \leq V_{C_2} \leq 0.1 \\ 1.0, & \text{if } V_{C_2} > 0.1 \end{cases}$$

where saturation current $I_S = 10.0 \text{ E-}6 \mu\text{A}$ and $V_T = 25 \text{ mV}$. Figs. 2 and 3 show typical chaotic waveforms and a projection of chaotic attractor obtained in numerical simulation of the model.

Although the appearance of chaos in the circuit can be explained within the continuous time model, it is not the most suitable model for the detailed analysis of chaotic dynamics of this circuit. Indeed, the conductance of the base-emitter junction $dg(V_{BE})/dV_{BE}$, which appears in front of the time derivative in equation (13) experiences sharp changes when the transistor opens and closes. It results in alternation of “fast” pulsations and “slow” oscillations. Due to the existence of such fast and slow motions in the circuit it seems more natural to describe these motions using separate sets of equations, which provide more precise description of the dynamical processes at each stage. One set of the equations describes the dynamics of fast pulsations when the transistor is closed. The other one describes slow oscillations when the transistor is open. Using this approach, we

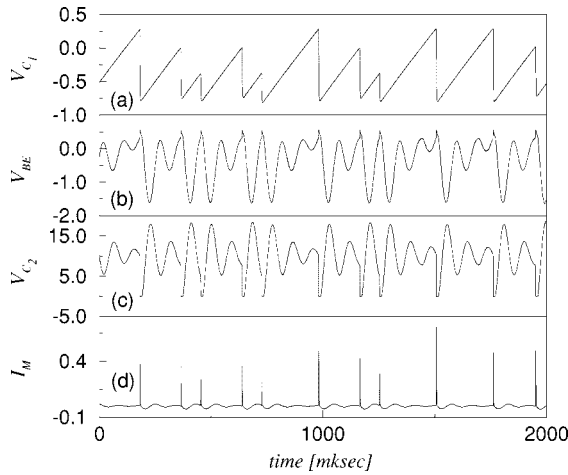


Fig. 2. Waveforms of chaotic oscillations obtained in numerical simulations of continuous time model (11)–(13) with the parameter values $V_{cc} = 10.3$, $C_1 = 47$ nF, $R_1 = 38.2$ k Ω , $C_2 = 3.9$ nF, $R_2 = 800$ Ω , $L_1 = 0.5$ mH, $k = 8$, and $h = 200$.

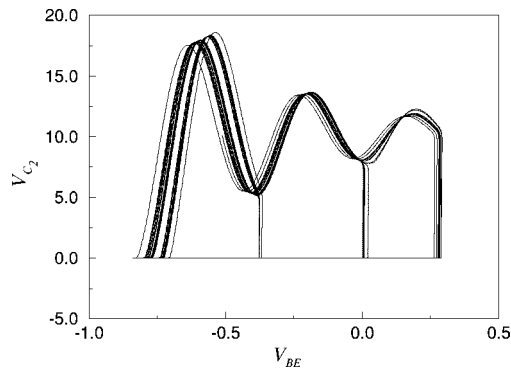


Fig. 3. Projection of the chaotic attractor onto the plane (V_{BE}, V_{C_2}) plotted for the oscillations shown in Fig. 2.

can derive a relatively simple map that provides a clear view on the origin of the chaos and its bifurcations.

III. 1-D MAP FOR THE CHAOTIC DYNAMICS OF THE CIRCUIT

Here, we consider the dynamics of the circuit as two alternating phases of evolution: fast, when transistor is closed, and slow, when transistor is open. To apply this approach we will describe the transistor as a switch. For the sake of simplicity the nonlinearities of the transistor will be modeled using piecewise-linear functions in the form

$$I_C = V_{C_2}/R_{CE}(V_{BE}) \quad (15)$$

$$R_{CE}(V_{BE}) = \begin{cases} \infty, & \text{if } V_{BE} \leq 0 \\ 0, & \text{if } V_{BE} > 0 \end{cases} \quad (16)$$

and

$$I_B(V_{BE}) = \begin{cases} 0, & \text{if } V_{BE} \leq 0 \\ V_{BE}/R_{BE}, & \text{if } V_{BE} > 0 \end{cases} \quad (17)$$

where R_{BE} is the resistance of the base-emitter junction of the transistor in a closed state. Below we will show using experimental studies that such simple approximation of the transistor operation is quite sufficient for description of the circuit dynamics in a wide range of the parameters. From the measurements of the inductance of the winding L_2 of the transformer T

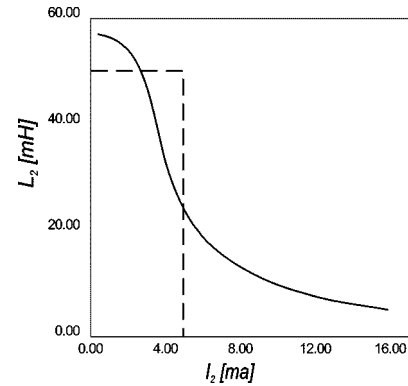


Fig. 4. Differential inductance the coil L_2 as a function of DC current (solid line) and it's approximation (dashed line).

we found that nonlinearity of this inductance is significant, see Fig. 4. We will take this nonlinearity in to account by describing the permeability of ferromagnetic core in the transformer as a piecewise-linear function

$$\mu(I_\mu) = \begin{cases} \mu_H, & \text{if } I_\mu \leq I_\mu^* \\ \mu_0, & \text{if } I_\mu > I_\mu^* \end{cases}, \quad \mu_H/\mu_0 \gg 1 \quad (18)$$

where μ_0 is the permeability of vacuum and I_μ^* is the critical number of ampere-turns (3) at which the saturation of permeability becomes significant. With such approximation the inductance of windings L_1 and L_2 , as well as mutual inductance M of the transformer are the piecewise-linear functions of I_μ .

A. Generation of Pulse

We begin the analysis of the circuit starting from the moment of time t_0 when voltage V_{BE} reaches the threshold level ($V_{BE} = 0$) and the transistor U closes. Taking into account that magnetic leakage flux is about zero, and assuming that current I_B is mostly the one recharging capacitor C_1 (in this case the current through resistor R_1 is much less than the current I_B), we can write the equations for the currents in the transformer in the form

$$L_T \frac{dI_\mu}{dt} + R_2 I_\mu = V_{cc} \quad (19)$$

$$I_B = \frac{M}{Z(p)} \frac{dI_\mu}{dt} \quad (20)$$

where $L_T = L_2(1 + R_2/k^2 Z(p))$ is the effective inductance of the transformer, $Z(p) = (1 + R_{BE}C_1 p)/(C_1 p)$ is the load impedance of transformer, $p = d/dt$ is differential operator, $k = n_2/n_1$, and $I_\mu = I_{L_2} - I_B/k$ is magnetization current.

It follows from the condition of continuity of the magnetization current that when transistor U closes, the magnetization current I_μ is equal to the value of current I_{L_2} which flew through the winding L_2 before the V_{BE} have reached the threshold. Solving (19) with the initial condition $I_\mu(t_0^+) = I_\mu(t_0^-) = I_{L_2}(t_0^-)$ we find the evolution of magnetization current in the form

$$I_\mu(t - t_0) = I_{\max} \left(1 - \left(1 - \frac{I_{L_2}(t_0^-)}{I_{\max}} \right) \right) e^{-(R_2(t-t_0)/L_T)} \quad (21)$$

where $I_{\max} = V_{cc}/R_2$. As it follows from (21) the magnetization current increases up to the value $I_{\mu} = I_{\mu}^*$ (we assume that $I_{\mu}^* < I_{\max}$) where the saturation in the core of transformer T becomes significant. As a result of saturation, the induced EMF in L_1 drops to zero and the transistor opens. Therefore, the duration τ_p of current pulse can be found from (21) using condition $I_{\mu}(\tau_p) = I_{\mu}^*$

$$\tau_p = \frac{L_T}{R_2} \ln \frac{I_{\max} - I_{L_2}(t_0^-)}{I_{\max} - I_{\mu}^*}. \quad (22)$$

During pulse generation the capacitor C_1 is recharged by current $I_B(t)$, and the voltage across C_1 becomes equal U . To evaluate this voltage we assume that the parameters of circuit were selected in such a way that $R_{BE}C_1 \gg \tau_p$ and $k \gg 1$. In this case $Z(p) \approx R_{BE}$, $L_T \approx L_2$, and

$$U = -\frac{M}{R_{BE}C_1} (I_{\mu}^* - I_{L_2}(t_0^-)). \quad (23)$$

B. Slow Evolution in the Time Interval Between Pulses

After the formation of pulse the transistor becomes open and current I_B becomes equal to zero. Now capacitor C_1 is "slowly" charged with the current through resistor R_1 . Therefore, after the pulse generation, the slow evolution of voltage V_{C_1} can be written in the form

$$V_{C_1}(t) = V_{cc} \left[1 - \left(1 + \frac{M}{V_{cc}R_{BE}C_1} \right) (I_{\mu}^* - I_{L_2}(t_0^-)) \right] e^{-(t/R_1C_1)}. \quad (24)$$

While the capacitor charges, the current in resonant circuit L_2C_2 can oscillate. The damping oscillations in this resonant circuit have the form

$$I_{L_2}(t) = I_{\mu}^* e^{-(R_2t/2L_2)} \cos \omega t \quad (25)$$

where $\omega = \sqrt{1/(L_2C_2) - R_2^2/(4L_2^2)}$. These oscillations induce EMF in the L_1 winding, which equals to

$$U_{L_1} = M dI_{L_2}/dt.$$

During the slow evolution of blocking oscillator, the voltage across base-emitter junction $V_{BE}(t) = U_{C_1}(t) + U_{L_1}$ increases till it reaches the threshold value [$V_{BE} = 0$, see (16), (17)] where the transistor opens and begins the generation of the next pulse. Therefore, the time interval t between two consecutive pulses generated in the oscillator can be found as a root of the following equation

$$V_{cc} \left[1 - \left(1 + \frac{M}{V_{cc}R_{BE}C_1} \right) (I_{\mu}^* - I_{L_2}(t_0^-)) \right] \cdot e^{-(t/R_1C_1)} - MI_{\mu}^* e^{-(R_2t/2L_2)} \cdot \left(\frac{R_2}{2L_2} \cos \omega t + \omega \sin \omega t \right) = 0. \quad (26)$$

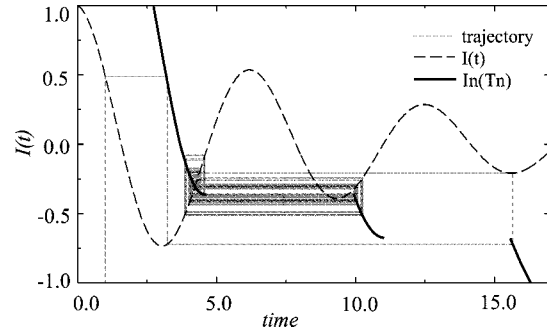


Fig. 5. Functions of the model map $I(t)$ and $I_n(T_{n+1})$ plotted for the parameter values $\alpha = 6.00$, $\beta = 0.22$, $\delta_c = 0.1$, and $\delta^{-1} = 63.0$. The trajectory of the map is shown by dotted line.

C. Model Map

The first root of (26) defines the time interval t_{n+1} between the n th and the $(n+1)$ th pulses as an implicit function of current $I_{L_2}(t_0^-) = i_n$, which was flowing in the resonant circuit L_2C_2 right before the beginning of generation of the n th pulse. On the other hand, (25) enable us to find the value of the current i_n as a function of the time interval t_n between the $(n-1)$ th and the n th pulses. Therefore, using (25) and the first root of (26), one can find a mapping for the dynamics of the time intervals t_n in the following form

$$t_{n+1} = F_1(i_n) \quad (27)$$

$$i_n = F_2(t_n). \quad (28)$$

Resolving (26) with respect to current $i_n = I_{L_2}(t_0^-)$ and taking into account (25) we will find the model map of the blocking oscillator as follows:

$$I_n = 1 + \alpha(1 - e^{\delta T_{n+1}}) + \alpha\beta(\delta_c \cos T_{n+1} + \sin T_{n+1})e^{(\delta - \delta_c)T_{n+1}} \quad (29)$$

$$I_n = e^{\delta_c T_n} \cos T_n \quad (30)$$

where $I_n = i_n/I_{\mu}^*$, $T_n = \omega t_n$. We also introduced new parameters

$$\delta = \frac{1}{R_1C_1\omega}$$

$$\delta_c = \frac{R_2}{2L_2\omega}$$

$$\alpha = \frac{R_{BE}C_1V_{cc}}{MI_{\mu}^*}$$

$$\beta = \frac{MI_{\mu}^*\omega}{V_{cc}}.$$

Fig. 5 presents a typical shape of functions (29), (30) and a chaotic trajectory of the map. The time interval T_{n+1} as a function of previous value of current I_n is found using (29). Note that the function $I_n = I_n(T_{n+1})$ given by (29) is not monotonous. As a result, (27) may have several roots T_{n+1}^k . Since the time interval T_{n+1} is a time which voltage V_{BE} needs to reach the threshold $V_{BE} = 0$, only the first root of (27) has a physical meaning. This is the reason why function $I_n(T_{n+1})$ plotted in Fig. 5 is discontinuous.

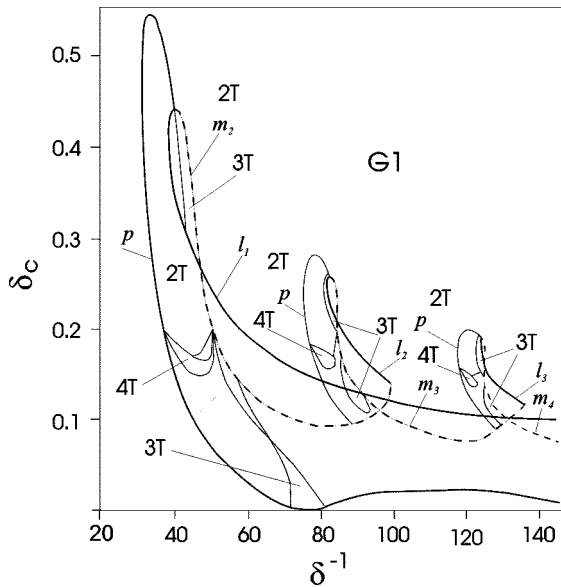


Fig. 6. Bifurcation diagram of the model map evaluated for the parameter values $a = 0.6$ and $b = 0.22$.

D. Bifurcations and Chaos in the Model Map

The simplicity of model maps (29), (30) enables one to perform a detailed analysis of bifurcation and specify the main bifurcation scenarios of the transition to chaotic behavior. The bifurcation diagram shown in Fig. 6 presents bifurcation curves in the parameter plane (δ^{-1} , δ_c) which specify the parameter regions with chaotic behavior. Note that fixed points of the map, which are located at the intersections if the nonlinear functions $I_n = F_1(T_{n+1})$ and $I(t)$ correspond to the of periodic pulsations of blocking oscillator.

Curve p corresponds to the bifurcation where the multiplier of the fixed point crosses the value minus one. Depending on the parameter δ_c this bifurcation can be supercritical or subcritical. In the first case, this bifurcation leads to the appearance of limit cycle with the period $2T$. In the second case it leads to the onset of chaotic oscillations. In Fig. 6 the regions corresponding to chaotic oscillations are filled with gray.

Curves marked with indexes m_i and l_i in Fig. 6 correspond to the parameters values where the fixed point disappear as the result of the bifurcation on border of the intervals where function $I_n = F_1(T_{n+1})$ has physical meaning. Since fixed points of the model map (29), (30) located at the intersection of functions $I_n = F_1(T_{n+1})$ and (28) they disappear when the intersection moves out of the interval thought the ether left border (shown by dotted curves m_i) or the right border (shown by dotted curves l_i), there index i stands for the interval counter.

It follows from the bifurcation diagram that when the dissipation in resonant circuit L_2C_2 characterized by parameter δ_c is small enough the model map demonstrate chaotic regime in a broad range of parameter δ .

IV. EXPERIMENT

The chaotic dynamics of the modified blocking oscillator was also studied in the experiment. For the experiment we built the circuit which diagram is shown in Fig. 1, where we added an

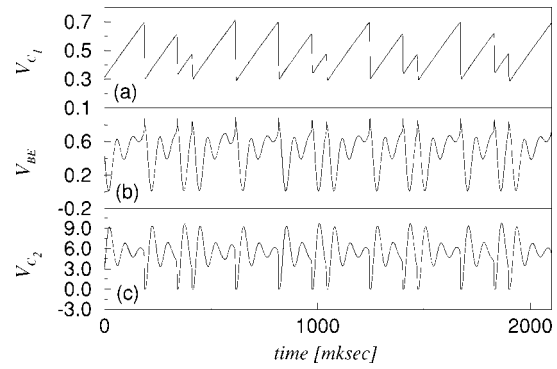


Fig. 7. Waveforms of chaotic oscillations measured in the experiment this the circuit. Parameters of the circuit are $V_{cc} = 6.0$ V, $C_1 = 47$ nF, $R_1 = 45.8$ k Ω , $C_2 = 3.9$ nF, $R_2 = 800$ Ω , $L_1 = 0.5$ mH, and $L_2 = 5.0$ mH.

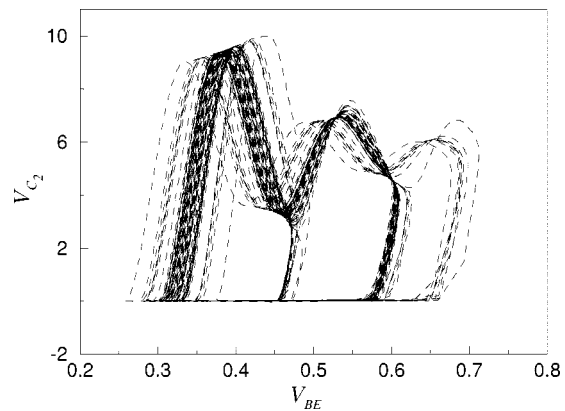


Fig. 8. Projection of the chaotic attractor onto the plane (V_{BE} , V_{C_2}) plotted using the waveforms shown in Fig. 7.

output transformer to generate output chaotic pulses. The first winding of this transformer was driven by collector current of the transistor. As one can see from the diagram the collector current is zero all the time except for short intervals of time when the transistor U is closed. The second winding of the output transformer was loaded to a 100 Ω resistor. Waveforms of the output pulses were measured at the resistor.

A. Chaos in the Circuit

The experiments show that the circuits can generate a large variety of chaotic regimes, which characterized by different numbers of the dumped oscillations in the resonant circuit between the consecutive pulse. Many of these chaotic regimes are well described by our continuous time model (11)–(13) and the model map. To demonstrate the similarity between the dynamics the continuous time model and the real circuit we tuned the circuit to the regime similar to the one obtained in the numerical simulations that is shown in Fig. 2. Fig. 7 presents chaotic waveform of the voltages measured in the experiment. Comparing these figures and the shapes of chaotic attractors presented in Figs. 3 and 8 one can see the similarity of the chaotic processes in the model and in the circuit.

Fig. 9 shows the parameters region (gray) that corresponds to the regime of chaotic pulsations of the circuit. Comparing figures Figs. 9 and 6, one can see that the locations of the bifurcation curves p and the structure of the region of chaotic behavior

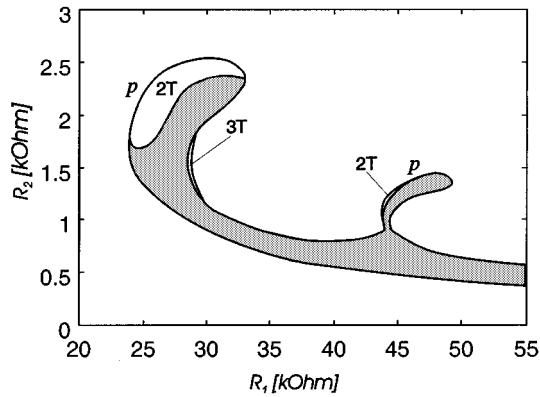


Fig. 9. Region of chaotic regimes on the plain of parameters (R_1 , R_2) and some bifurcation curves measured in the experiment with chaotic blocking oscillator. Parameters of the circuit are $V_{cc} = 6.0$ V, $C_1 = 47$ nF, $C_2 = 3.9$ nF, $L_1 = 0.5$ mH, and $L_2 = 5.0$ mH.

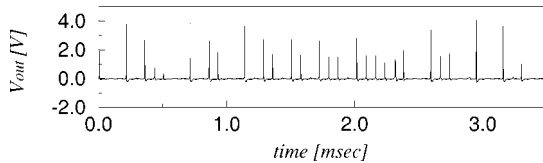


Fig. 10. The of the output chaotic pulse signal V_{out} measured at the output transformer loaded with 100Ω resistor.

measured in the circuit have some similarity with the bifurcation diagram obtained for the model map. The presented experimental diagram does not show detailed structure of bifurcations which are very dense in the vicinity of the region with chaotic dynamics. In the experiment, we also could not follow the bifurcations of stable limit cycles of long period. They can disappear due to the small noise and the specific features of the circuit. Indeed the influence of this noise becomes essential when voltage V_{BE} gets close to the threshold value.

Despite the difference in the details of the numerical and experimental bifurcation diagrams, the region of the chaotic behavior in both cases has similar structure in the shape of sequences of tongues. In both cases, chaos is observed when the parameter of the dissipation in the L_2C_2 circuit becomes sufficiently low. Therefore, we can conclude that simple one-dimensional map (29), (30) correctly describes main processes in the circuit, and can be used to explain the origin of chaotic behavior of the blocking oscillator.

B. Generation of Chaotic Pulse Signals

Operating in the regime of chaotic oscillations the transistor U closes for the short time intervals, which results in the generation of short pulses of current through the collector. The rest of the time, the transistor U is open and the collector current is zero. Using the output transformer we transform these pulses of the collector current into the output voltage signal in the resistive load. Fig. 10 shows a waveform of the output chaotic pulse signal measured from the circuit operating in the regime of oscillations presented in Figs. 7 and 8.

The important feature of the chaotic blocking oscillator is that such circuit provides simple means for generation of a very broad-band chaotic signal. The spectrum of the output signal

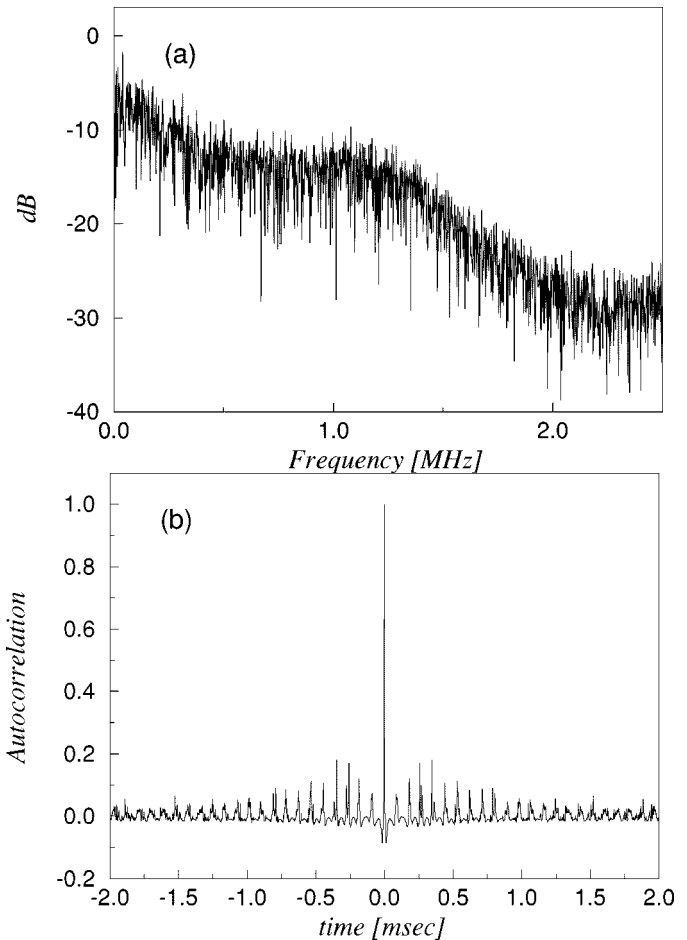


Fig. 11. The spectrum (a) and autocorrelation function (b) of the output chaotic pulse signal shown in Fig. 10.

and its autocorrelation function is shown in Fig. 11. The width of the main peak in the autocorrelation function equals to the double width of the generated pulses. The maximal amplitude of the other peaks in the function depends on the complexity of chaotic regime of oscillations and on Q -factor of the resonant circuit C_2L_2 .

V. CONCLUSIONS

We have studied the nonlinear dynamics of blocking oscillator with additional capacitor in the collector circuit and have shown the dynamical origin for the appearance chaotic pulsations in the oscillator. The additional capacitor C_2 and the inductance of the transformer T form a resonant circuit that leads to appearance of damped oscillations in the collector circuit while the transistor is open. Using continuous time model and simplified one-dimensional (1-D) map model we have shown that such oscillator can start to behave chaotically if the next pulse of the blocking oscillator fires before the oscillations in the resonant circuit are over.

Concluding this paper, we would like to note that the considered modification of classical blocking oscillator circuit is not the only one that leads to the onset of chaotic behavior of the oscillator. For example, chaos in the classical blocking oscillator circuit may be achieved by connecting an additional capacitor between V_{cc} and the collector of transistor U .

REFERENCES

- [1] R. N. Madan, Guest Ed., *Chua's Circuit: A Paradigm for Chaos*. Singapore: World Scientific, 1993.
- [2] V. Ya. Kislov, N. N. Zalogin, and Ye. A. Myasin, "Study of stochastic self-oscillatory processes in self-excited oscillators with delay," *Radio Eng. Electron. Phys.*, vol. 24, no. 6, pp. 92–101, 1979.
- [3] S. V. Kyashko, A. S. Pikovskii, and M. I. Rabinovich, "Self-exciting oscillator for the radio-frequency range with stochastic behavior," *Radio Eng. Electron. Phys.*, vol. 25, no. 2, pp. 74–79, 1980.
- [4] V. S. Anishchenko, V. V. Astakhov, and T. E. Letchford, "Experimental study of the structure of a strange attractor in a model generator with a nonlinear inertial term," *Sov. Phys.—Tech. Phys.*, vol. 28, no. 1, pp. 91–92, 1983.
- [5] Yu. V. Gulyaev, A. S. Dmitriev, and V. D. Kislov, "Strange attractors in ring-type self-oscillating systems," *Sov. Phys.—Dokl.*, vol. 30, no. 5, pp. 360–361, 1985.
- [6] F. O'Caibre, G. M. Maggio, and M. P. Kennedy, "Devaney chaos in an approximate one-dimensional model of the Colpitts oscillator," *Int. J. Bifurcation Chaos*, vol. 7, no. 11, pp. 2561–2568, 1997.
- [7] P. A. Bernhardt, "Coupling of the relaxation and resonant elements in the autonomous chaotic relaxation oscillator (ACRO)," *Chaos*, vol. 2, no. 2, pp. 183–199, 1992.
- [8] A. R. Volkovskii, "Chaotic blocking oscillator," in *Proc. 3rd Int. Specialist Workshop on Nonlinear Dynamics of Electronic Systems. NDES '95*, M. P. Kennedy, Ed. Dublin, 1995, pp. 263–266.
- [9] N. F. Rulkov and A. R. Volkovskii, "Threshold synchronization of chaotic relaxation oscillations," *Phys. Lett.*, pt. A, vol. 179, no. 4–5, pp. 332–336, 1993.
- [10] H. Torikai, T. Saito, and W. Schwarz, "Synchronization via multiplex pulse trains," *IEEE Trans. Circuits Syst. I*, vol. 46, pp. 1072–1085, Sept. 1999.
- [11] T. Morie, S. Sakabayashi, M. Nagata, and A. Iwata, "Nonlinear function generators and chaotic signal generators using a pulse-width modulation method," *Electron. Lett.*, vol. 33, no. 16, pp. 1351–1352, 1997.
- [12] T. Yang and L. O. Chua, "Chaotic impulse radio: A novel chaotic secure communication system," *Int. J. Bifurcation Chaos Appl. Sci. Eng.*, vol. 10, no. 2, pp. 345–357, 2000.
- [13] M. Sushchik, N. Rulkov, L. Larson, L. Tsimring, H. Abarbanel, K. Yao, and A. Volkovskii, "Chaotic pulse position modulation: A robust method of communicating with chaos," *IEEE Commun. Lett.*, vol. 4, pp. 128–130, Apr. 2000.
- [14] A. A. Andronov, A. A. Vitt, and S. E. Khaikin, *Theory of Oscillations*. New York: Pergamon, 1966.



Nikolai F. Rulkov received the M.S. degree in 1983 and Ph.D. degree in 1991, both in physics and mathematics, from the University of Nizhny Novgorod, Nizhny Novgorod, Russia.

In 1983, he joined the Radio Physics Department of the University of Nizhny Novgorod, where he was a Researcher until 1993. Since, 1993, he has been with the Institute for Nonlinear Science, University of California, San Diego. His research interests are in the areas of bifurcation theory, nonlinear phenomena, theory of synchronization, chaos and applications of

chaotic oscillations in science and engineering.



Alexander R. Volkovskii was born in Nizhny Novgorod, Russia, in 1961. He received the M.S. and Ph.D degrees in radiophysics, both from Lobachevskii State University, Nizhny Novgorod, Russia, in 1983 and 1994, respectively.

From 1994, he was a Research Scientist and later an Assistant Professor at the Radiophysics Department, Lobachevskii State University. Currently, he is a Researcher at the Institute for Nonlinear Science, University of California, San Diego. His scientific interests include nonlinear dynamics and chaos in electronic circuits and computer simulations.